Available online at www.ijpsdr.com

International Journal of Pharmaceutical Sciences and Drug Research
2017; 9(4): 201-209

Research Article

ISSN: 0975-248X
CODEN (USA): IJPSPP

In Silico Validation of Anti-tuberculosis Activity in *Andrographis paniculata* (Burm.F.) Nees

Nimmi Haridas, S Sreekumar*, C.K Biju

Biotechnology and Bioinformatics Division, Saraswathy Thangavelu Centre, Jawaharlal Nehru Tropical Botanic Garden and Research Institute, Puthenthope, Thiruvananthapuram, Pin 695 586, Kerala, India

ABSTRACT

Tuberculosis is an infectious disease caused by *Mycobacterium tuberculosis*. Although drugs are available for its treatment, administrations of those drugs have so many limitations and emergence of drug resistant strains of bacteria necessitate for the discovery of novel drugs. Plants are the best source of novel drugs and they are safe to use. *Andrographis paniculata* has been used in the Indian traditional medicine against tuberculosis, however, its efficacy was not tested and chemical molecules having the drug property are not identified. In the present investigation a total 140 chemical molecules derived from *A. paniculata,* 114 compounds collected from databases and 26 compounds determined through GC-MS analysis, were docked with three target proteins such as filamentous temperature sensitive protein Z (FtsZ), decaprenyl phosphoryl-beta D ribofuranose 2 epimerase (DprE1) and pantothenate kinase (PanK) and based on the lowest binding energy (≤-5kcal/mol) hit molecules were identified. Further hydrogen bond interaction and drug-likeness property analysis revealed that the compound β-sitosterol have inhibitory activity against FtsZ and DprE1. The compound 3,14 dideoxyandrographolide/andrograpanin showed least binding energy with PanK protein. The toxicity and drug-likeness property analysis indicated that among the hit molecules β-sitosterol is a promising lead molecule for the development of anti-tuberculosis drug. The results also substantiate the traditional use of this plant against tuberculosis.

Keywords: *In silico*, docking, *Andrographic paniculata,* Tuberculosis, *Mycobacterium*.

DOI: 10.25004/IJPSDR.2017.090408 **Int. J. Pharm. Sci. Drug Res. 2017; 9(4): 201-209**

***Corresponding author**: Dr. S. Sreekumar
Address: Senior Scientist, Biotechnology and Bioinformatics Division, Saraswathy Thangavelu Centre, Jawaharlal Nehru Tropical Botanic Garden and Research Institute, Puthenthope, Thiruvananthapuram 695 586, Kerala, India
E-mail ✉: drsreekumar@rediffmail.com
Relevant conflicts of interest/financial disclosures: The authors declare that the research was conducted in the absence of any commercial or financial relationships that could be construed as a potential conflict of interest.
Received: 27 June, 2017; **Revised:** 10 July, 2017; **Accepted**: 13 July 2017; **Published:** 24 July 2017

INTRODUCTION

Tuberculosis (TB) is continuing as an infectious major killer disease along with HIV. According to World Health Organisation (WHO) 10.4 million new TB cases were reported globally in 2015. Of these, 2.8 million were from India and global annual death rate due to TB

is 1.5 million. [1] It is caused by a group of closely related bacterial species *viz. Mycobacterium tuberculosis* complex and in humans it is caused by *Mycobacterium tuberculosis.* [2] Bacillus Calmette–Guérin (BCG) vaccination is the only preventive measure and administration of more than one antibiotics in combination for long period (6-12 months) induces serious side effects and poor compliance by the patients. Emergence of multi-drug resistant (MDR) and extensively-drug resistant (XDR) strains of *M. tuberculosis* is the major problem now a-days. [3] In these backdrops, there is an urgent need to find out novel drugs against TB for addressing the forgoing problems.

Plants are always synthesizing novel molecules with therapeutic properties and serve as renewable source of drug molecules. The drugs derived from natural sources induce fewer or no side effects and safe to use. India has a rich repository of plant genetic diversity which can synthesize unique bioactive molecules and such plants are widely used in the Indian traditional systems of medicine for the treatment of various diseases including tuberculosis. But its efficacy and mode of molecular mechanism of drug action are seldom scientifically demonstrated due to several reasons such as complexity and instability of chemical constituents in herbal extracts, scarcity of plant material, high investment and time consuming, etc. Application of bioinformatics tools is the best option to circumvent these problems for preliminary evaluation of drug activity in plants. The present investigation was aimed to validate the anti-tuberculosis activity and identification of lead molecules in *Andrographis paniculata* through *in silico* screening method.

MATERIALS AND METHODS

Collection and Extraction of Plant Sample

The mature leaves of *Andrographis paniculata* collected from the field grown plants conserved in the medicinal plant conservatory, Saraswathy Thangavelu Centre, JNTBGRI, Puthenthope, Thiruvananthapuram were shade dried at room temperature, grinded and made as fine powder. Twenty five gram of this powder was subjected to soxhlet extraction with 250 ml hexane for 6 hours, the extract was further concentrated using rotary evaporator until the solvent was completely exhausted and stored in air tight bottles.

GC-MS Analysis

The analysis of samples was performed using a Varian CP-3800 gas chromatograph with a varian saturn 2200 mass spectrometer. The GC-MS is equipped with a VF-5MS fused silica capillary column (30 m × 0.25 mm × 0.25µm varian). Helium was used as carrier gas with a flow rate of 1mL/min. The injection volume for each sample was 1µL delivered by syringe with a split less mode for 45 seconds before being vented. The temperature in the inlet and transfer line was at 280°C. The temperature of the oven was initially at 50°C for 1.5 minutes followed by a ramp to 300°C at 5°C/min with a final hold time of 10 minutes giving a total run time of 40 minute. Electron impact ionization (70eV) was utilized with a quadrapole mass analyzer operated in full scan mode (40-600 m/z).

Preparation of Target Proteins

The three dimensional (3D) structures of the selected target proteins such as filamentous temperature sensitive protein Z (FtsZ PDB id: 2Q1X), decaprenylphosphoryl-β-D-ribose 2′-epimerase (DprE1 PDB id: 4FDO) and pantothenate kinase (PanK PDB id: 4BFS) were retrieved from the Protein Data Bank (PDB). [4] The physical and chemical parameters of the selected protein targets were analyzed using the tool ProtParam. [5] The sequence data of the target proteins were subjected to BLASTp against human genome. [6] The citrate ligand bound to the FtsZ protein, the 3-nitro-N-[(1R)-1-phenylethyl]-5-(trifluoromethyl) benzamide and flavin-adenine dinucleotide present in DprE1 and n-[1-(5-{[2-(4-fluorophenoxy) ethyl]sulfanyl}-4-methyl-4h-1,2,4-triazol-3-yl)ethyl]-2-(trifluoromethyl) benzamide present in PanK were removed prior to docking. The active site of the target proteins were predicted using MetaPocket. [7]

Preparation of Ligands

Perusal of literature and search on open access chemical databases, information on 114 phytochemicals present in *A. paniculata* were collected. In addition, 33 phytochemicals were identified through GC-MS analysis. Canonical SMILES of the 79 molecules were obtained from the chemical database Pubchem. [8] Structures of remaining 61 molecules were drawn using the tool ChemSketch. The 3D structures in .pdb format of all phytochemicals were generated using the software tool CORINA. [9]

Docking

Docking experiments were carried out using the tool AutoDock 4.2 which is an automated molecular docking software package, following the standard procedure. [10] Water molecules present in the protein molecules were removed and added polar hydrogen. Root of the ligand molecules and the torsions were selected. All torsions of the ligand were allowed to rotate. In the protein molecule torsions were checked for the selected residues. Precalculated grid maps required for running the program were calculated using the Autogrid program. The grid was positioned at the macromolecule with XYZ co-ordinates set at -6.164, 53.402,-0.146 respectively and grid point spacing of 0.375 Å for FtsZ protein. Similarly for DprE1 protein, the XYZ co-ordinates were set at 3.028, 3.333, -0.278 respectively and grid point spacing of 0.375 Å. For PanK protein the XYZ co-ordinates were set at -19.056, -55.849 and -12.702 respectively. Grid calculations were used to determine the total interaction energy for a ligand with a macromolecule. The docking calculations were done by keeping all the docking parameters at default value. A total of 10 GA runs were done with a population size of 150 and 25×105 evaluations were done with 27000 iterations. The mutation rate and cross over rate were set at 0.02 and 0.80 respectively. A global

local search method based on Lamarckian Genetic Algorithm (LGA) which is the most efficient, reliable and successful when compared to other algorithms was selected to calculate the best conformers.

Molecular Property Analysis

Molecular properties of the compounds were analyzed by using drug-likeness and molecular property prediction tool hosted by MolSoft L.L.C. The tool uses Partial Least Square regression model for calculation. It predicts LogP, LogS, polar surface area, volume and drug-likeness score of the given compound. [11]

Molecular Visualization and Interaction Analysis

The docked structures were visualized using the software PyMol. [12] Interaction between the protein and ligand molecule was analyzed using LigPlot. The tool generates diagrams showing both hydrogen bond and hydrophobic interactions. [13]

Toxicity Prediction

ADME and toxicity were analyzed using the web based prediction tool PreADMET. The tool can predict ADME, toxicity and drug-likeness properties of chemical molecules. [14]

RESULTS AND DISCUSSION

Preparation of Ligand Molecules

Of the 140 phytochemicals selected for screening 114 were already reported from *A. paniculata* and the remaining 26 were determined through GC-MS analysis. A total 33 compounds were identified from the mature leaves hexane extract of *A. paniculata* through GC-MS analysis (Table 1 & Figure 1.). Of these, only 26 compounds were selected for docking because the remaining seven compounds showed degree of freedom of torsion angle beyond 32, which is not fit for docking. As followed earlier [15] the 3D structures of all compounds were generated in .pdb format and used for further docking.

Table 1: Compounds identified from *Andrographis paniculata* through GC-MS analysis of hexane extract

S. No	Compound Name	RT value	Area %
1.	Cyclopentanol, 1-methyl	3.858	0.49
2.	3-Carene	6.969	0.008
3.	Cyclohexene, 4-methylene	8.203	0.008
4.	Camphene	9.675	0.10
5.	Linalylisobutyrate	11.723	0.009
6.	Bicyclo[2.2.1]heptan-2-one	12.872	0.002
7.	Bicyclo[2.2.1]heptan-2-ol	13.366	0.17
8.	3-Cyclohexen-1-ol, 4-met	13.484	0.003
9.	alpha.-Cubebene	15.757	0.04
10.	Phenol, 2-methoxy-4-(2-p	15.936	0.34
11.	Epizonarene	16.121	0.22
12.	Cyclobuta[1,2:3,4]dicycl	16.219	0.09
13.	2-Azatricyclo[3.3.1.0(3,	16.545	1.73
14.	gamma.-HIMACHALENE	16.688	0.33
15.	1,4,7,-Cycloundecatriene	17.015	0.05
16.	Naphthalene, 1,2,3,4,4a,	17.148	0.03
17.	Bicyclo[4.4.0]dec-1-ene,	17.244	0.13
18.	Azulene, 1,2,3,4,5,6,7,8	17.333	0.07
19.	Gitoxigenin	18.182	0.11
20.	2,6,6,9,2',6',6',9'-Octa	18.808	0.23
21.	E-11-Methyl-12-tetradece	19.878	0.11
22.	Dibenz(a,h)acridine	20.169	1.06
23.	Dibenz(a,c)acridine	20.488	0.45
24.	Molybdenum, tetrakis(.et	20.931	0.71
25.	2-[p-Methoxyphenyl]-8-me	21.436	0.06
26.	Aspidospermidine-3-carbo	21.738	0.09
27.	Tritetracontane	22.236	0.15
28.	Tetrapentacontane, 1,54-	22.834	0.45
29.	Tertbutyloxyformamide, N	23.436	0.77
30.	1-Hexacosene	24.043	0.92
31.	1-Hentetracontanol	25.267	0.73
32.	Phosphoric acid, triborn	25.415	0.27
33.	Cholesta-22,24-dien-5-ol	30.541	0.02

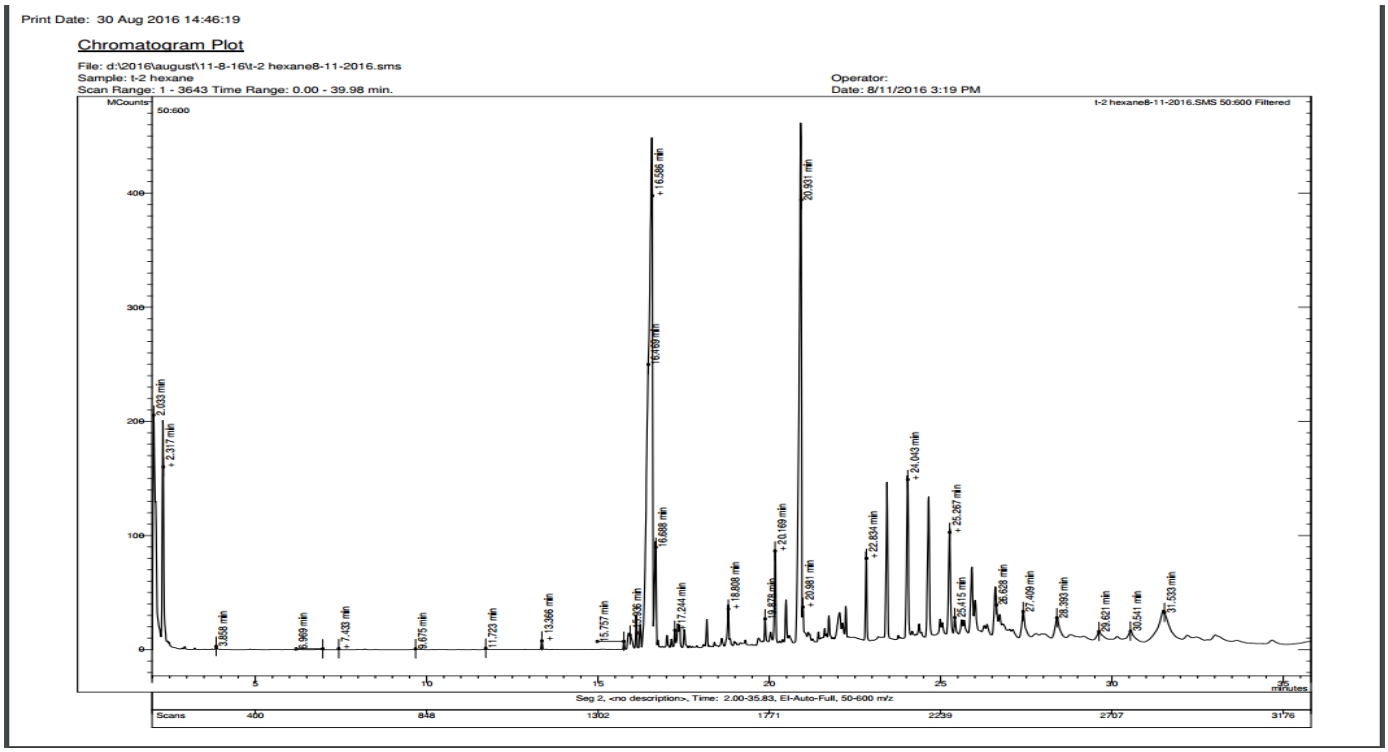

Fig. 1: Chromatogram of GC MS analysis of hexane extract of *A.paniculata*

Table 2: Docking results of phytochemicals from *Andrographis paniculata* and the target proteins FtsZ, DprE1and PanK

S. No	Phytochemicals	FtsZ	DprE1	PanK
1.	(-)-3betahydroxy-5-stigmata-9(11),22(23)diene	-6.70	-8.80	-3.54
2.	1,2-dihydroxy-6,8-dimethoxyflavone	-5.70	-6.63	-7.03
3.	1,4,7,-cycloundecatriene, 1,5,9,9-tetram	-5.53	-6.66	-7.09
4.	1,8-dihydroxy-3,7-dimethoxyflavone	-5.46	-6.98	-6.71
5.	13,14,15,16-tetranorentlabd-8(17)ene-3,12,19triol	-4.60	-6.84	+2.45
6.	14-acety-l3,19-isopropylideneandrographolide	-5.88	-9.74	-6.08
7.	14-acetylandrographolide	-6.51	-8.80	+0.51
8.	14-alpha-lipoyl-andrographolide	-5.46	-4.25	+23.75
9.	14-deoxy-11,12-dehydroandrographolide	-6.20	-8.29	-3.13
10.	14-deoxy-11,12-didehydroandrographiside	-7.03	-6.12	+5.72
11.	14-deoxy-11-hydroxy andrographolide	-5.47	-5.69	-1.69
12.	14-deoxy-11-oxo andrographolide	-6.60	-8.62	-7.25
13.	14-deoxy-12-hydroxy andrographolide	-6.23	-8.28	-4.44
14.	14-deoxy-12-methoxy andrographolide	-5.94	-7.37	-2.69
15.	14-deoxy-14,15-dehydroandrographolide	-6.16	-8.83	-6.69
16.	14-deoxy-15-isopropylidine11,12-didehydroandrographolide	-5.60	-9.86	-1.46
17.	14-deoxy-17-hydroxy andrographolide	-6.19	-7.71	-4.95
18.	14-deoxyandrographolide	-5.08	-6.89	-5.33
19.	18-andrographiside	-5.36	-6.44	+2.01
20.	19-hydroxy3oxoentlabda8(17),11,13trien16,15olide	-6.40	-6.37	-3.55
21.	19-o-acetylanhydroandrographolide	-5.82	-9.01	-4.65
22.	1-hexacosene	-5.48	-6.40	-3.25
23.	1-hydroxy-3,7,8-trimethoxyxanthone	-5.67	-7.29	-6.57
24.	2-(2'benzyloxy)benzoyloxy-3,4,6-trimethoxyacetophenon	-4.29	-6.44	-5.46
25.	2-(4-methoxyphenyl)-8-methylquinoline-4-carboxylic acid	-4.46	-7.52	-7.36
26.	2',5-dihydroxy-7,8-diimethoxyflavone-2'-o-beta(d)glucoside	-5.19	-6.91	-3.48
27.	2,6,6,9,2',6',6',9'-octamethyl-[8,8']bi[	-5.40	-9.72	+22.81
28.	2-hydroxy-3,4,6,2'-tetramethoxy benzoyl methane	-5.07	-7.79	-7.43
29.	2hydroxy5,7,8-trimethoxyflavone	-4.88	-7.48	-6.21
30.	3,14dideoxyandrographolide/andrograpanin	-6.36	-9.09	-8.36
31.	3,15,19trihydroxyentlabda8(17),13-dien-16-oic acid	-4.08	-9.23	-5.31
32.	3,18,19trihydroxyentlabda8(17),13dien16,15olide	-5.37	-7.27	-5.82
33.	3,19dihydroxy14,15,16trinorentlabda8(17),11-dien-13-oic acid	-4.11	-6.95	-7.37
34.	3,19dihydroxyentlabda8(17),12-dien-16,15-olide	-6.16	-8.78	-5.57
35.	3,19-isopropylidene-andrographolide	-5.93	-9.02	-7.38
36.	3',2',5,7-tetramethoxyflavone	-5.20	-8.45	-5.87
37.	3,3',5,5',7-pentahydroxyflavanone	-4.99	-7.67	-6.01
38.	3,4-dicaffeoylquinicacid	-4.14	-5.93	+21.29
39.	3,7,8,2'-tetramethoxy5hydroxyflavone	-4.11	-5.25	-5.24
40.	3,7,8-trimethoxy-1-hydroxyxanthone	-5.19	-6.90	-6.98
41.	3-carene	-5.47	-5.21	-5.45
42.	3-Cyclohexen-1-ol, 4-methyl-1-(1-methyle/Terpinen-4-ol	-5.69	-4.16	-4.61
43.	4,8-dihydroxy-2,7-dimethoxyflavone	-4.70	-6.77	-6.77
44.	4-hydroxy-2-methoxy cinnamaldehyde	-4.36	-5.09	-5.98
45.	4'-hydroxy-7,8,2',3'-tetramethoxyflavone-5-betadglucopyranosyl-oxyflavone	-4.35	-5.68	-3.56
46.	5,2',6-'trihydroxy-7-methoxyflavone-2'-O-betadglucopyranoside	-5.28	-5.81	+8.31
47.	5,2'-dihydroxy-7,8-dimethoxyflavone or skullcapflavone	-4.87	-5.01	+7.22
48.	5,2'-dihydroxy-7,8-dimethoxyflavone-3'-betadglucopyranosyl oxyflavone	-4.99	-6.59	+3.56
49.	5,3'-dihydroxy-7,8,4'-trimethoxyflavone	-4.62	-6.88	-6.36
50.	5,4'-dihydroxy-7,8,2',3'-tetrametoxyflavone	-3.65	-5.69	+6.87
51.	5,5'-dihydroxy-7,8,2'-trimethoxyflavone	-5.29	-7.60	-6.40
52.	5,7,2',3'-tetramethoxyflavanone	-4.86	-8.01	-6.00
53.	5,7,8,2'-tetramethoxyflavone	-5.61	-8.11	-6.07
54.	5,7,8-trimethoxy-2'-hydroxyflavone	-5.10	-8.18	-5.68
55.	5-hydroxy 7,8-dimethoxyflavanone	-5.14	-7.23	-6.60
56.	5-hydroxy-2'-betadglucosil-oxy-7-methoxyflavone	-5.03	-6.94	+1.20
57.	5-hydroxy-7,2',3'-trimethoxyflavone	-4.64	-7.40	-5.65
58.	5-hydroxy-7,2',6'-trimethoxyflavone	-5.39	-7.67	-6.88
59.	5-hydroxy-7,8,2',3'-tetramethoxyflavone	-4.66	-7.52	-4.16
60.	5-hydroxy-7,8,2',6'-tetramethoxyflavone	-5.12	-5.87	-3.63
61.	5-hydroxy-7,8,2'3'4-pentamethoxyflavone	-4.48	-7.43	-3.65
62.	5-hydroxy-7,8,2'-trimethoxyflavone	-5.29	-7.45	-3.94
63.	6'-acetylneoandrographolide	-6.78	-7.03	-5.12
64.	7,8,2'-trimethoxyflavone-5-betaglucopyranosyl-oxyflavone	-4.73	-5.27	+11.94
65.	7,8-dimethoxyflavone-5-betadglucopyranosyl-oxy-flavone	-4.57	-6.87	+0.60
66.	7-o-methylwogonin	-4.98	-7.10	-6.36
67.	α cubebene	-6.23	-7.13	-5.31
68.	α-sitosterol	-8.34	-10.18	+32.33
69.	Andrograpanin	-5.26	-6.58	+36.45
70.	Andrograpanolide	-5.11	-5.24	+19.25
71.	Andrographidinea	-5.21	-6.01	+3.11

Table 2: Docking results of phytochemicals from *Andrographis paniculata* and the target proteins FtsZ, DprE1and PanK

S. No	Phytochemicals	FtsZ	DprE1	PanK
72.	Andrographidineb	-3.96	-6.33	-6.20
73.	Andrographidinec	-5.49	+23.34	-6.26
74.	Andrographidined	-5.26	-5.85	-6.41
75.	Andrographidinee	-5.89	-5.83	-3.58
76.	Andrographidinef	-3.88	-3.72	+55.26
77.	Andrographin	-5.35	-3.14	+9.14
78.	Andrographiside	-6.08	-6.94	+2.25
79.	Andrographolide	-5.81	-8.77	-4.86
80.	Andrographoneo	+1.11	+23.34	+73.42
81.	Andrographoside	-4.53	-8.19	+16.12
82.	Andropanoside	-4.41	-6.35	+1.37
83.	Apigenin	-5.59	-6.81	-6.28
84.	Apigenin_7_o_b_d_glucoside_	-5.23	-5.78	+0.81
85.	Apigenin-5,7,4'-trihydroxyflavone/apigenin	-4.45	-6.81	-6.33
86.	Apigenin-7,4'-dimethylether	-4.69	+5.93	-5.86
87.	Aspidospermidine-3-carboxylic acid, 2,3	-6.64	-8.41	-7.32
88.	Azulene, 1,2,3,4,5,6,7,8-octahydro-1,4-d/ Alphaguaiene	-5.85	-7.10	-6.82
89.	β- daucosterol	-5.64	-5.52	+68.21
90.	β -sitosterolglucoside	-6.69	-5.64	+683.49
91.	Bicyclo[2.2.1]heptan-2-ol, 1,7,7-trimeth/Borneol	-4.34	-4.98	-4.39
92.	Bicyclo[2.2.1]heptan-2-one, 1,7,7-trimet/camphor	-4.20	-5.45	-4.71
93.	Bicyclo[4.4.0]dec-1-ene, 2-isopropyl-5-m	-5.90	-6.54	-7.40
94.	Bisandrographolide A	+3.56	+4.11	+3.22
95.	Bisandrographolide B	+15.36	-1.55	+2.89
96.	Bisandrographolide C	+6.38	+9.22	+6.14
97.	Bisandrographolide ether	+20.38	+64.79	+308.47
98.	β-sitosterol	-8.39	-10.26	+8.71
99.	Caffeicacid	-3.85	-5.77	-5.17
100.	Camphene	-4.31	-5.03	-5.18
101.	Carvacrol	-4.89	-5.36	-5.90
102.	Chlorogenic-acid	-3.55	-5.91	-3.70
103.	Cinnamic-acid	-3.52	-5.51	-5.45
104.	Cyclobuta[1,2:3,4]dicyclopentene, decahy/Betabourbonene	-5.12	-7.18	-6.70
105.	Cyclohexene, 4-methylene-1-(1-methylethy	-4.83	-5.02	-5.83
106.	Cyclopentanol, 1-methyl	-3.74	-4.11	-3.95
107.	Deoxyandrographiside	-6.82	-1.10	-6.46
108.	Deoxyandrographolide	-6.45	-7.28	+0.04
109.	Dibenz(a,c)acridine	-6.72	-8.44	-6.99
110.	Dibenz(a,h)acridine	-6.52	-8.35	-7.35
111.	Dicaffeol acid	+2.15	-4.89	+3.55
112.	E-11-methyl-12-tetradecen-1-ol acetate	-3.73	-5.03	-4.99
113.	Ent-14-betahydroxy-8(17),12labadiene16,15-olide-3-beta-19-oxide	-6.79	-9.21	-6.83
114.	Entlabda8(17),13diene15,16,19triol	-5.46	-6.85	-6.01
115.	Epizonarene	-6.29	-6.82	-7.42
116.	Ergosterol peroxide	-3.56	-2.55	-3.69
117.	Eugenol	-4.58	-4.36	-5.52
118.	Ferulic acid	-3.92	-5.41	-5.33
119.	Gamma.-himachalene	-5.50	-7.08	-7.71
120.	Gitoxigenin	-6.64	-8.84	-5.95
121.	Hentriacontane	-0.56	+2.58	+20.27
122.	Isoandrographolide	-5.90	-7.77	-4.46
123.	Linalylisobutyrate	-5.87	-5.59	-5.41
124.	Myristic acid	-3.15	-6.25	-4.36
125.	Naphthalene, 1,2,3,4,4a,5,6,8a-octahydro	-5.29	-6.64	-7.73
126.	Neoandrographolide	-6.66	-7.37	+7.68
127.	Oleanolic acid	-5.36	-8.01	+10.36
128.	Onysilin	-6.53	-2.25	-5.67
129.	Oroxylin A	-6.03	-7.16	-6.30
130.	Panicolin	-4.92	-3.84	-6.47
131.	Paniculide A	-5.32	-6.94	-7.05
132.	Paniculide B	-4.77	-6.77	-7.13
133.	Paniculoside I	-4.37	+2.49	+18.34
134.	Phenol, 2-methoxy-4-(2-propenyl)-, aceta	-5.30	-5.54	-6.19
135.	Quinic acid	-2.99	-4.91	-3.91
136.	Stigmasterol	-9.47	-5.12	+9.15
137.	T-butoxyformamid, n-methyl-n-[4-(1-pyrrolidinyl)-2-butynyl]-	-5.79	-5.11	-4.94
138.	Tritricontane	-1.24	-4.58	+0.86
139.	Wightionolide	-5.22	-7.89	-5.04
140.	Wogonin	-5.43	-7.34	-4.17

Table 3: Molecular interaction details of selected lead molecules with three target proteins

Target Protein	Phytochemicals	ΔG_{bind}	Hbond	H bond residues	Bond length	Hydrophobhic interactions
FtsZ	β-sitosterol	-8.39	O-H-O	ASP178	2.91	ARG26, LEU166, MET169, GLY170, ASP171, VAL174, ASP178, ARG181, SER182, GLU185, VAL186, ASN189, ILE 225
	α-sitosterol	-8.34	O-H-O	ASP178	2.69	LEU166, VAL174, PHE133, SER182, ASP178, ARG181, ARG26, GLU185, MET169, LEU167, GLY170
	14deoxy11,12didehydroandrographiside	-7.03	O-H-O O-H-O N-H-O N-H-O N-H-O	SER182 ASP178 ARG181 ARG26 ARG26	2.47 3.35 2.85 2.99 2.90	LEU167, LEU166, ALA179, ASP178, ARG181, ARG26, GLU185, VAL186, ILE225, GLY170, MET169
	Deoxyandrographiside	-6.82	N-H-O N-H-O O-H-O O-H-O	ARG181 ARG181 ASP178 SER182	3.03 2.81 3.02 2.65	VAL174, ILE225, ALA179, LEU167, VAL186, MET169, GLU185, ARG26, ARG181, ASP178, SER182, GLY170, LEU166
	Ent14betahydroxy8(17),12labadiene16,15olide3beta19oxide	-6.79	O-H-O	ALA179	2.92	ILE225, ASN189, VAL186, SER182, MET169, LEU166, VAL174, LEU167, GLY170, GLU185
DprE1	β-sitosterol	-10.26	O-H-O O-H-O	GLY 117 LEU 317	3.09 3.25	PHE369, TYR415, ALA179, TYR60, GLY133, TYR314, GLY321, THR118, LYS418, PRO116, GLN336, LEU115, VAL365, LYS134, HIS132
	α-sitosterol	-10.18	N-H-O N-H-O	GLY117 THR118	2.87 2.89	LYS367, PHE366, LEU317, TYR314, LEU115, GLY133, SER228, PRO116, GLY117, THR118, LYS418, LYS134, GLN336, VAL365, HIS132
	14deoxy15isopropylidine11,12didehydroandrographolide	-9.86	O-H-O O-H-O N-H-O O-H-O	LEU115 HIS132 HIS132 TYR415	2.92 2.74 2.97 2.80	GLY117, TYR314, PRO116, LYS134, GLY133, HIS132, ILE131, TYR415, ALA417, ARG58, GLN336, VAL365, LEU317, CYS387, LEU115, LYS418
	14acetyl3,19isopropylideneandrographolide	-9.74	O-H-O	TYR415	2.84	CYS129, ALA417, ILE131, TYR415, HIS132, ASN385, LEU317, VAL365, LYS367, SER228, TYR314, LYS134, GLN336, LYS418
	Stigmasterol	-9.47	O-H-O	PRO116	3.00	LYS134, LYS367, LEU317, GLY117, LYS418, THR118, ARG58, VAL121, PRO116, ILE131, TYR415, ALA417, GLN336, GLY133, PHE369, SER228
PanK	3,14dideoxyandrographolide	-8.05	O-H-O N-H-O N-H-O	LYS147 VAL99 ASN280	2.82 3.02 2.61	VAL99, ASN280, LEU203, GLY148, LYS147, TYR182, ILE272, ILE276, ILE285, SER98, ASN277
	Naphthalene, 1,2,3,4,4a,5,6,8a-octahydro	-7.73	Nil	Nil	Nil	TRP273, ILE285, VAL99, LEU281, ASN277, SER98, LYS147, GLY148, ASN280, PHE149, ILE272, TYR235, ILE276
	Gamma.-himachalene	-7.71	Nil	Nil	Nil	ASN277, ILE272, ILE276, GLY148, PHE149, ASN280, LYS147, TYR235, VAL99, TRP273
	Epizonarene	-7.42	Nil	Nil	Nil	LEU203, ASN280, LEU281, SER98, VAL99, ILE285, TYR235, ASN277, ILE272, TRP273, ILE276, LYS147, GLY148
	Bicyclo[4.4.0]dec-1-ene, 2-isopropyl-5-m	-7.40	Nil	Nil	Nil	ILE285, SER98, VAL99, TYR235, TRP273, ILE272, ASN277, ASN280, LYS147, ILE276, GLY148

Selection of Target Protein

The target protein FtsZ is a bacterial tubulin homolog which plays a key role in bacterial cell division. [16-17] In the presence of guanosine triphosphate (GTP), FtsZ polymerizes bidirectionally at the centre of the cell on the inner membrane to form a highly dynamic helical structure known as the Z-ring. The recruitment of several other cell division proteins lead to Z-ring formation and eventually cell division. [18] Unlike other bacteria, the mechanism of septum formation in *Mycobacterium tuberculosis* (Mtb) is yet to be well demonstrated. Another potential target selected was Decaprenylphosphoryl-β-D-ribose 2′-epimerase (DprE1), an enzyme involved in the formation of decaprenylphosphoryl-D-ribose to decaprenylphosphoryl-D-arabinose (DPA), the sole donor of mycobacterial cell wall content arabinan. [19] It is also essential for the *in vitro* growth of bacteria. [20] Next target was pantothenate kinase (PanK, type I), an enzyme which catalyses the rate limiting step of cofactor Coenzyme A (CoA) pathway. Three types of PanK based on biochemical and structural characteristics difference were described. *M. tuberculosis* type I PanK (*Mt*PanK), is the only PanK gene essential for bacterial growth *in vitro* and *in vivo.* [21]

Analysis of Target Proteins

FtsZ is a dimer protein that undergoes lateral association and crystallizes into an arc like dimer. [18] It is a single chain of protein consists of 379 amino acid residues with a theoretical pI value of 4.55 and an average hydropathicity of 0.119. It has two folds, tubulin nucleotide binding domain (residues 8-205) and bacillus chorismatemutase domain (residues 206-312) and 15 helices and 11 strands. The active site of the protein consists of 15 amino acid residues. DprE1 is a

monomer protein composed of 481 amino acid residues. It is having a theoretical pI value of 7.17 and average hydropathicity of -0.147. DprE1 has FAD binding domain comprising of residues 7-196 and 413 to 461 with two beta sheets and many alpha helices. Substrate binding domain with residues 197 to 412 consist of anti parallel beta sheets and three alpha helices. [22-23] The active site of the protein was well defined with 35 residues. The PanK is a cyclic homo-2-er with 318 amino acid residues. It has a pI value of 7.47 and average hydropathicity value of -0.249. Secondary structure analysis showed 17 helices and 13 beta strands in the protein structure. The structure of the protein was extensively studied and found that all the inhibitors bind to a common binding site. The target molecule incorporates a triazole inhibitory molecule which was found to be forming hydrogen bond interactions with residues ASN277 and TYR235. The BLASTp analysis indicated that the sequence similarity of all the three selected target molecules with human genome was insignificant.

Docking Analysis

Docking calculations were done to analyse the binding affinity of phytochemicals with the selected target proteins. Molecules with ΔG_{bind} ≤-5kcal/mol were selected as hit molecules. Out of 140 phytochemicals docked with three target proteins, 85, 117 and 70 molecules showed ΔG_{bind}≤-5kcal/mol against target proteins FtsZ, DprE1 and PanK respectively and can be considered as hit molecules. It is interesting to note that 41 hit molecules have binding affinity with all the three targets (Table 2).

Among the 85 hit molecules against FtsZ protein, top five molecules with least free energy of binding were selected as lead molecules for further analysis. They are β-sitosterol (-8.39 kcal/mol), α-sitosterol (-8.34 kcal/mol), 14deoxy11, 12didehydroandrographiside (-7.03 kcal/mol), deoxyandrographiside (-6.82 kcal/mol) and Ent14betahydroxy8 (17), 12labadiene16, 15olide3beta19oxide (-6.79 kcal/mol). Further hydrogen bond interaction analysis of the docked structure of FtsZ showed that the compound β-sitosterol and α-sitosterol established hydrogen bond interaction with ASP178. The ligand 14deoxy11, 12didehydroandrographiside showed five hydrogen bond interactions with SER182, ASP178, ARG181, ARG26 and ARG26 and deoxyandrographiside formed four hydrogen bond interactions with ARG181, ARG181, ASP178 and SER182. The compound ent14betahydroxy8 (17), 12labadiene16, 15olide 3beta19oxide which represent the lead molecule with highest ΔG_{bind} showed only a single bond with the residue ALA179. Based on the interaction analysis β-sitosterol was selected as the best lead against FtsZ (Figure 2) because of its least free energy of binding, ideal drug-likeness score and non-mutagenic quality of the compound (AmesTest).

Similarly against DprE1, of the 117 hit molecules having ΔG_{bind} ≤ -5kcal/mol the compounds β-sitosterol (-10.72 kcal/mol), α-sitosterol (-10.18 kcal/mol), 14deoxy15isopropylidine11, 12didehydro andrographolide (-9.86 kcal/mol), 14acetyl3, 19isopro pylideneandrographolide (-9.74 kcal/mol) and stigmasterol (-9.47 kcal/mol) showed least free energy of binding. The compound β-sitosterol showed two hydrogen bond interactions with active residues, GLY117 and LEU317. The GLY117 was the binding site of the inhibitor molecule nitroso-benzothiazinone.

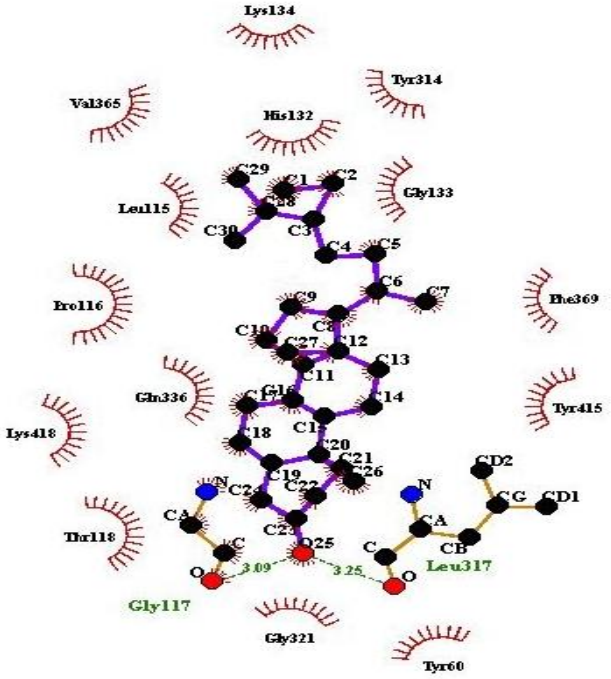

Fig. 2: Hydrogen and hydrophobic interaction of β-sitosterol with active residues of DprE1

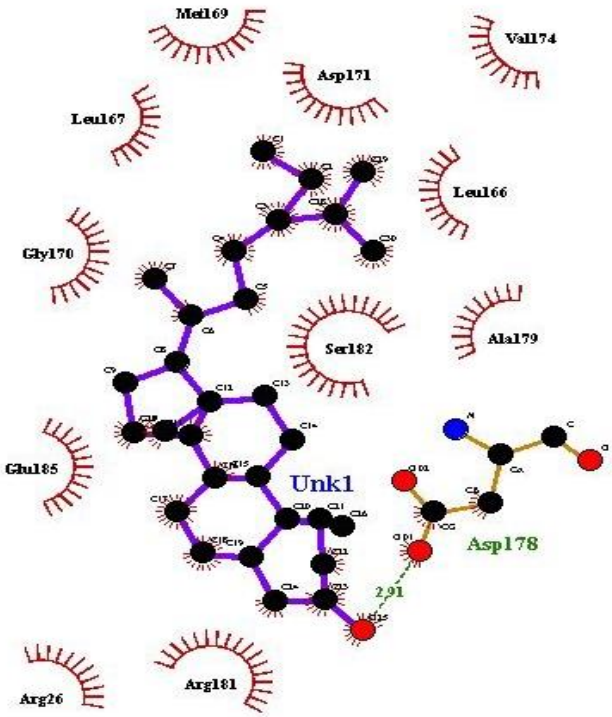

Fig. 3: Hydrogen and hydrophobic interaction of β-sitosterol with active residues of FtsZ

Table 4: Molecular property analysis of the lead molecules calculated using MOLSOFT

Target Protein	Hits with $\Delta G_{bind} \leq$-7kcal/mol	Molecular formula	Molecular weight	HBA	HBD	MolLogP	MolLogS	MolPSA	No. of stereo isomers	Drug likeness model score
FtsZ	β-sitosterol	$C_{29}H_{50}O$	414.39	1	1	9.48*	-7.51	16.28	9	0.88
	α-sitosterol	$C_{30}H_{50}O$	426.39	1	1	9.84*	-6.98	16.17	9	0.55
	14-deoxy11, 12didehydroandrographiside	$C_{26}H_{38}O_9$	494.25	9	5	0.99	-2.36	118.38	10	-0.07
	Deoxyandrographiside	$C_{26}H_{40}O_9$	496.27	9	5	1.14	-2.53	118.38	10	0.14
	Ent14betahydroxy8(17),12labadiene16,15olide3beta19oxide	$C_{20}H_{28}O_4$	332.20	4	1	2.92	-4.01	47.55	6	-0.65
DprE1	β-sitosterol	$C_{29}H_{50}O$	414.39	1	1	9.48*	-7.51	16.28	9	0.88
	α-sitosterol	$C_{30}H_{50}O$	426.39	1	1	9.84*	-6.98	16.17	9	0.55
	14-deoxy15isopropylidine11, 12didehydroandrographolide	$C_{26}H_{38}O_9$	494.25	9	5	0.99	-2.36	118.38	10	-0.07
	14-acetyl3,19-isopropylideneandrographolide	$C_{25}H_{36}O_6$	432.25	6	0	3.94	-3.76	58.26	6	-0.37
	Stigmasterol	$C_{29}H_{48}O$	412.37	1	1	8.82*	-7.71	16.28	9	0.73
PanK	3,14-dideoxyandrographolide	$C_{20}H_{30}O_3$	318.22	3	1	4.47	-3.90	39.54	4	-0.31
	Naphthalene, 1,2,3,4,4a,5,6,8a-octahydro	$C_{15}H_{24}$	204.19	0	0	5.24*	-3.93	270.89	3	-1.09
	Gamma.-himachalene	$C_{15}H_{24}$	204.19	0	0	5.42*	-4.45	292.50	2	-1.10
	Epizonarene	$C_{15}H_{24}$	204.19	0	0	4.90	-4.45	275.05	2	-0.77
	Bicyclo[4.4.0]dec-1-ene, 2-isopropyl-5-m	$C_{15}H_{24}$	204.19	0	0	5.31*	-4.22	268.10	2	-1.05

α-sitosterol also formed two hydrogen bond interactions with active site residue GLY117 and THR118.

14deoxy15isopropylidine11,12didehydroandrographolide formed four hydrogen bond interactions with LEU115, HIS132, HIS132, and TYR415. The compounds 14acetyl 3, 19 isopropylideneandrographolide and stigmasterol formed single hydrogen bond interaction with residues TYR415 and PRO116 respectively. β-sitosterol with least free energy of binding and two hydrogen bond interaction was selected as best lead against DprE1 (Figure 3).

Out of 70 hit molecules identified against PanK the compounds 3,14 dideoxy andrographolide/ andrograpanin (-8.05 kcal/mol), naphthalene, 1,2,3,4,4a,5,6,8a-octahydro (-7.73 kcal/mol), γ-himachalene (-7.71 kcal/mol), epizonarene (-7.42 kcal/mol) and bicyclo[4.4.0]dec-1-ene, 2-isopropyl-5-m (-7.40 kcal/mol) were selected as top hits as they showed strong binding affinity and least free energy of binding against the target. Molecular interaction analysis of the docked compounds revealed that 3,14 dideoxyandrographolide established three hydrogen bonds while 2-hydroxy3, 4, 6, 2'tetramethoxy benzoyl methane have a single hydrogen bond (LYS147). All other selected hit molecules showed no hydrogen bond interaction. None of the hits qualifies as lead molecule as they showed poor drug- likeness score and positive mutagenic properties. Interaction of hit molecules and molecular property analysis of hits were given in Table 3 and Table 4.

Analysis of the docked results showed that the compound β-sitosterol have inhibitory activity against two of the selected target proteins FtsZ and DprE1. Although the compound showed violation of Lipinski's rule of Five (1 violation), it has promising drug-likeness score. Ames test done using PreADMET tool, revealed that β-sitosterol is non-mutagenic, not cytotoxic or genotoxic compound. [24] Long term administration of β-sitosterol did not exhibit toxicity and accumulate in the tissues of test animals. [25] β-sitosterol is a white crystalline compound, with a molecular formula of $C_{29}H_{50}O$. It is one of the major phytosterol found in plants. Structure of the compound includes a steroidal skeleton with both five membered and six membered rings. The side chain consists of 10 carbons and a methyl substitution at the 21st position and ethyl substitution at the 24th position which marks the difference of the compound with cholesterol. [26] Synthesis of β-sitosterol can be from two pathways - deoxyxylulose and mevalonate pathway. Cycloartenol was identified as the substrate for synthesizing the compound. The absorption and distribution of β-sitosterol in human was similar to that of cholesterol but it is not easily esterified as cholesterol. [27-28] Pharmacologically the compound was active against colon carcinoma cell lines and breast cancer. It can prevent renal carcinogenesis and modulates signal transduction pathways. Dietary supplement of sitosterol was found to be effective in lowering the cholesterol levels. The compound has immunomodulatory, analgesic, anti-mutagenic, anti-inflammatory, anti-diabetic, anti-pyretic, angiogenic, anti-fertility, anti-microbial and anti-complementary activities. Oral administration of β-sitosterol was found to enhance neural stem cell proliferation. [29] β-sitosterol activates mitochondrial membrane potential, leading to increased activity in skeletal muscles. [30]

The present study showed that β-sitosterol has significant inhibitory action against the two target proteins of *M. tuberculosis*, FtsZ and DprE1. None of the molecules against PanK can be considered for further analysis as they showed low drug-likeness properties. Further *in vitro* and *in vivo* studies are essential to

substantiate the inhibitory activity of β-sitosterol against *Mycobacterium tuberculosis*.

ACKNOWLEDGEMENT

We thank Department of Science and Technology, Govt. of India, New Delhi for providing INSPIRE fellowship, Director, JNTBGRI, and Dr. T. Madhan Mohan, Advisor, DBT for their supports and encouragements

REFERENCE

1. WHO. Global tuberculosis report. Geneva: World Health Organization, 2016.
2. Sandhu GK. Tuberculosis: Current situation, challenges and overview of its control programs in India. J Global Infect Dis. 2011; 1(3):143.
3. Rustomjee R, Lockhart S, Shea J, Fourie PB, Hindle Z, Steel G, Hussey G, Ginsberg A, Brennan MJ. Novel licensure pathways for expeditious introduction of new tuberculosis vaccines: A discussion of the adaptive licensure concept. Tuberculosis. 2014; 31(94):178-82.
4. Bernstein FC, Koetzle TF, Williams GJ, Meyer Jr EF, Brice MD, Rodgers JR, Kennard O, Shimanouchi M, Tasumi M. The Protein Data Bank: A computer-based archival file for macromolecular structures. J Mol Biol. 1977; 112:535-542.
5. Gasteiger E, Hoogland C, Gattiker A, Wilkins MR, Appel RD, Bairoch A. Protein identification and analysis tools on the ExPASy server. In The Proteomics Protocols Handbook. Humana Press. 2005, pp.571-607.
6. Altschul SF, Gish W, Miller W, Myers EW, Lipman DJ. Basic local alignment search tool. J Mol Biol. 1990; 215:3403-410.
7. Huang B. MetaPocket: A meta approach to improve protein ligand binding site prediction. OMICS A Journal of Integrative Biology. 2009; 1(13):325-30.
8. Bolton EE, Wang Y, Thiessen PA, Bryant SH. PubChem: Integrated platform of small molecules and biological activities. Annu Rep Comput Chem. 2008; 31(4):217-41.
9. Sadowski J, Gasteiger J, Klebe G. Comparison of automatic three-dimensional model builders using 639 X-ray structures. J Chem Inf Comput Sci. 1994; 34(4):1000-1008.
10. Morris GM, Huey R, Lindstrom W, Sanner MF, Belew RK, Goodsell DS, Olson AJ. Autodock4 and AutoDockTools 4: Automated docking with selective receptor flexibility. J. Computational Chemistry. 2009; 16:2785-91.
11. http://www.molsoft.com/mpropdesc.html (accessed 1 December, 2016).
12. DeLano WL. Pymol: An open-source molecular graphics tool. CCP4 Newsletter on Protein Crystallography. 2002; 40:82-92.
13. Wallace AC, Laskowski RA, Thornton J M. LIGPLOT: A program to generate schematic diagrams of protein-ligand interactions. Protein Eng. 1996; 8:127-134.
14. Lee SK, Lee IH, Kim HJ, Chang GS, Chung JE, No KT. "The PreADME Approach: Web-based program for rapid prediction of physico-chemical, drug absorption and drug-like properties". In EuroQSAR 2002 Designing Drugs and Crop Protectants: processes, problems and solutions. Blackwell Publishing. 2003, pp. 418-420.
15. Haridas N, Sreekumar S, Biju CK. Validation of Anti-Tuberculosis Activity and Identification of Leads in *Alstonia scholaris* L.(R. Br.). IOSR J Pharm Biol Sci. 2016; 11:12-19.
16. Slayden RA, Knudson DL, Belisle JT. Identification of cell cycle regulators in *Mycobacterium tuberculosis* by inhibition of septum formation and global transcriptional analysis. Microbiology. 2006; 152(6):1789-1797.
17. Löwe J, Amos LA. Crystal structure of the bacterial cell-division protein FtsZ. Nature. 1998; 391(6663):203-206.
18. Leung AK, White EL, Ross LJ, Reynolds RC, DeVito JA, Borhani DW. Structure of *Mycobacterium tuberculosis* FtsZ reveals unexpected, G protein-like conformational switches. J Mol Biol. 2004; 17(342):953-70.
19. Mikušová K, Huang H, Yagi T, Holsters M, Vereecke D, D'Haeze W, Scherman MS, Brennan PJ, McNeil MR, Crick DC. Decaprenylphosphorylarabinofuranose, the donor of the D-arabinofuranosyl residues of *Mycobacterial arabinan*, is formed via a two-step epimerization of decaprenylphosphoryl ribose. J Bacteriol. 2005; 1(187):8020-5.
20. Christophe T, Jackson M, Jeon HK, Fenistein D, Contreras-Dominguez M, Kim J, Genovesio A, Carralot JP, Ewann F, Kim EH, Lee SY. High content screening identifies decaprenyl-phosphoribose 2′ epimerase as a target for intracellular antimycobacterial inhibitors. PLoS Pathog. 2009; 30(10):e1000645.
21. Awasthy D, Ambady A, Bhat J, Sheikh G, Ravishankar S, Subbulakshmi V, Mukherjee K, Sambandamurthy V, Sharma U. Essentiality and functional analysis of type I and type III pantothenate kinases of *Mycobacterium tuberculosis*. Microbiology. 2010; 1(156):2691-701.
22. Batt SM, Jabeen T, Bhowruth V, Quill L, Lund PA, Eggeling L, Alderwick LJ, Fütterer K, Besra GS. Structural basis of inhibition of *Mycobacterium tuberculosis* DprE1 by benzothiazinone inhibitors. Proc Natl Acad Sci. 2012; 10(109):11354-9.
23. Bhutani I, Loharch S, Gupta P, Madathil R, Parkesh R. Structure, dynamics, and interaction of *Mycobacterium tuberculosis* (Mtb) DprE1 and DprE2 examined by molecular modeling, simulation, and electrostatic studies. PloS one. 2015; 19(10):e0119771.
24. Paniagua-Pérez R, Madrigal-Bujaidar E, Reyes-Cadena S, Molina-Jasso D, Gallaga JP, Silva-Miranda A, Velazco O, Hernández N, Chamorro G. Genotoxic and cytotoxic studies of beta-sitosterol and pteropodine in mouse. Biomed Res Int. 2005; 3:242-7.
25. Shipley RE, Peeiffer RR, Marsh MM, Anderson RC. Sitosterol Feeding. Circ Res. 1958; 1:373-82.
26. Behrman EJ, Gopalan V. Cholesterol and plants. J Chem Educ. 2005; 1(82):1791.
27. Gould RG. IV. Absorbability of beta-sitosterol. Trans. N. Y. Acad. Sci. 1955; 1:129-34.
28. Salen G, Ahrens Jr EH, Grundy SM. Metabolism of β-sitosterol in man. J Clin Invest. 1970; 49(5):952.
29. Bin Sayeed MS, Karim SM, Sharmin T, Morshed MM. Critical analysis on characterization, systemic effect, and therapeutic potential of beta-sitosterol: A plant-derived orphan phytosterol. Medicines. 2016; 15(3):29.
30. Wong HS, Leong PK, Chen J, Leung HY, Chan WM, Ko KM. β-sitosterol increases mitochondrial electron transport by fluidizing mitochondrial membranes and enhances mitochondrial responsiveness to increasing energy demand by the induction of uncoupling in C2C12 myotubes. J Funct Foods. 2016; 31(23):253-60.

HOW TO CITE THIS ARTICLE: Haridas N, Sreekumar S, Biju CK. *In Silico* Validation of Anti-tuberculosis Activity in *Andrographis paniculata* (Burm.F.) Nees. Int. J. Pharm. Sci. Drug Res. 2017; 9(4): 201-209. **DOI: 10.25004/IJPSDR.2017.090408**